Mapping of human brown adipose tissue in lean and obese young men

Brooks P. Leitner[a,1], Shan Huang[a,b,1], Robert J. Brychta[a], Courtney J. Duckworth[a], Alison S. Baskin[a], Suzanne McGehee[a], Ilan Tal[c], William Dieckmann[d], Garima Gupta[e], Gerald M. Kolodny[c], Karel Pacak[e], Peter Herscovitch[d], Aaron M. Cypess[a,2], and Kong Y. Chen[a,2,3]

[a]Diabetes, Endocrinology, and Obesity Branch, Intramural Research Program, National Institute of Diabetes and Digestive and Kidney Diseases, National Institutes of Health, Bethesda, MD 20892; [b]Department of Endocrinology and Metabolism, Huashan Hospital, Fudan University, Shanghai, 200032, China; [c]Division of Nuclear Medicine and Molecular Imaging, Department of Radiology, Beth Israel Deaconess Medical Center, Harvard Medical School, Boston, MA 02215; [d]Department of Positron Emission Tomography, National Institutes of Health, Bethesda, MD 20892; and [e]Eunice Kennedy Shriver National Institute of Child Health and Human Development, National Institutes of Health, Bethesda, MD 20892

Edited by Stephen O'Rahilly, University of Cambridge, Cambridge, United Kingdom, and approved June 7, 2017 (received for review March 30, 2017)

Human brown adipose tissue (BAT) can be activated to increase glucose uptake and energy expenditure, making it a potential target for treating obesity and metabolic disease. Data on the functional and anatomic characteristics of BAT are limited, however. In 20 healthy young men [12 lean, mean body mass index (BMI) 23.2 ± 1.9 kg/m^2; 8 obese, BMI 34.8 ± 3.3 kg/m^2] after 5 h of tolerable cold exposure, we measured BAT volume and activity by ^{18}F-labeled fluorodeoxyglucose positron emission tomography/computerized tomography (PET/CT). Obese men had less activated BAT than lean men (mean, 130 vs. 334 mL) but more fat in BAT-containing depots (mean, 1,646 vs. 855 mL) with a wide range (0.1–71%) in the ratio of activated BAT to inactive fat between individuals. Six anatomic regions had activated BAT—cervical, supraclavicular, axillary, mediastinal, paraspinal, and abdominal—with 67 ± 20% of all activated BAT concentrated in a continuous fascial layer comprising the first three depots in the upper torso. These nonsubcutaneous fat depots amounted to 1.5% of total body mass (4.3% of total fat mass), and up to 90% of each depot could be activated BAT. The amount and activity of BAT was significantly influenced by region of interest selection methods, PET threshold criteria, and PET resolutions. The present study suggests that active BAT can be found in specific adipose depots in adult humans, but less than one-half of the fat in these depots is stimulated by acute cold exposure, demonstrating a previously underappreciated thermogenic potential.

brown fat | PET/CT | obesity | metabolism

Long-term positive energy balance is the primary cause of the worldwide pandemic of obesity and diabetes. Excessive energy storage associated with obesity is accumulated principally in white adipose tissue (WAT). Conversely, brown adipose tissue (BAT) is a thermogenic tissue responsible for producing energy in the form of heat (1). In contrast to the homogeneous classical BAT seen in rodents, human BAT is composed of stromal tissue, white adipocytes (2, 3), and uncoupling protein-1 (UCP1)-containing thermogenic adipocytes of two different lineages (4): "brown" (5) and "beige (2)/brite" (6). BAT takes up plasma glucose and free fatty acids in response to mild cold exposure (7–9). It has been suggested that BAT activity may contribute to changes in energy expenditure, thus making it a potential target for the treatment of metabolic diseases (10).

To better understand human BAT in vivo, it is important to quantify both its volume and its metabolic activity. A common method for studying human BAT is by positron emission tomography (PET) and computed tomography (CT) imaging, using tissue density information from CT to identify adipose tissue and 2-deoxy-2-(^{18}F)fluoro-D-glucose (^{18}F-FDG) uptake to gauge its metabolic activity (11). Although commonly used, PET/CT-based BAT analysis involves several challenges (12): (*i*) human BAT is typically distributed in narrow fascial layers among muscle groups, organs, and bones of various densities and activities in the upper thorax; (*ii*) PET/CT coregistration is nontrivial and contains errors owing to differences in image resolution, patient motion, and partial volume effects (13); and (*iii*) normalization of the ^{18}F-FDG standardized uptake value (SUV) to body weight may be inappropriate (14). Although many researchers have moved beyond simple identification of the presence or absence of BAT (15), region of interest (ROI) methodologies (16) and the utility of SUV as a measure of BAT activity (17) vary substantially among investigators (9). Each of these issues can yield substantial discrepancies in BAT measurements. Given the lack of consensus on the methodological approaches to quantifying BAT by PET/CT, comparing findings is challenging. Thus, there is a knowledge gap regarding the amount of BAT present in adults and whether maximizing its volume and metabolic activity could impact human physiology.

The goal of the present study was to describe BAT's anatomic distribution and functional capacity in lean and obese healthy young men under tolerable cold exposure. Image processing techniques were used to investigate the impact of body composition normalization to quantify tracer uptake, ROI selection methods, and PET resolution on observed BAT quantification.

Significance

Brown adipose tissue (BAT) is currently being explored as a target for the treatment of obesity and diabetes after repeated demonstrations on positron emission tomography-computed tomography (PET/CT) imaging of its ability to metabolize glucose following acute cold exposure. Measurement of whole-body BAT volume, activity, and distribution is difficult because brown adipocytes are structurally commingled among white adipose tissue, muscle, and blood vessels. Thus, BAT's potential contribution to metabolism remains unclear. To address this, we have identified several refinements to improve current PET/CT analyses and demonstrated their impact in healthy lean vs. obese individuals. Using the refined technique, we defined whole-body BAT distribution and estimated its metabolic capacity and found that it is substantially higher than usually reported.

Author contributions: R.J.B. and K.Y.C. designed research; B.P.L., S.H., R.J.B., C.J.D., A.S.B., S.M., W.D., G.G., K.P., P.H., and K.Y.C. performed research; I.T., W.D., G.M.K., P.H., and K.Y.C. contributed new reagents/analytic tools; B.P.L., S.H., R.J.B., I.T., A.M.C., and K.Y.C. analyzed data; and B.P.L., S.H., R.J.B., W.D., A.M.C., and K.Y.C. wrote the paper.

The authors declare no conflict of interest.

This article is a PNAS Direct Submission.

Freely available online through the PNAS open access option.

[1]B.P.L. and S.H. contributed equally to this work.

[2]A.M.C. and K.Y.C. contributed equally to this work.

[3]To whom correspondence should be addressed. Email: chenkong@niddk.nih.gov.

This article contains supporting information online at www.pnas.org/lookup/suppl/doi:10.1073/pnas.1705287114/-/DCSupplemental.

An atlas of BAT ("BATlas") was composed that defines the anatomic distribution of activated BAT in terms of its relative volume and activity in each region capable of supporting brown or beige/brite adipocytes ("brownable"). We further identified the anatomic limits of each adipose depot for the accommodation of thermogenic adipocytes. Our findings suggest that the anatomic distribution and glucose uptake capacity of human BAT have been underappreciated, which has significant implications for determining its physiological roles.

Results

Demographics. Twenty young healthy male volunteers [12 lean, body mass index (BMI) 18.5–25 kg/m^2; 8 obese, BMI 30–40 kg/m^2] were admitted to the National Institutes of Health's Clinical Center for an inpatient study as a part of an Institutional Review Board-approved protocol (Clinical Trial identifier: NCT01568671). During each study day, subjects wore one pair of undershorts, one sleeveless form-fitting cotton shirt, one pair of form-fitting shorts, and one pair of light socks, for a combined thermal insulation value of 0.36 clo (a measure of clothing insulation). The subjects were exposed to varied ambient temperatures between 16.0 and 31.0 °C (in a randomized order) for 5 h daily over 13 d. On the final day, they remained at their lowest tolerable nonshivering cold temperature preceding ^{18}F-FDG PET/CT imaging. Compared with lean subjects, the obese subjects had a lower lean body mass percentage (LBM%), as measured by dual-energy X-ray absorptiometry (DXA; Lunar iDXA; GE Healthcare), and older age (Table 1).

LBM-Corrected SUV Equalizes ^{18}F-FDG Uptake Values in Non-BAT Tissues. Calculations using the SUV are the most commonly used approach to quantifying BAT metabolic activity and are often reported to describe the function of other tissues as well (12, 18). Therefore, we investigated the influence of body composition on metabolically active tissue SUVs. The SUV calculated based on total body mass (TBM) showed that lean subjects had lower SUVmean values in the skeletal muscle, liver, and cerebellum compared with obese subjects (Fig. 1*A*); however, when adjusted for LBM, using $SUV_{LB} = SUV^*(LBM\%)$, the SUV_{LB} values of all three tissues became comparable between the 2 groups (Fig. 1*B*). Because this adjustment confirmed the assumption that obese and lean muscle, liver, and cerebellum do not metabolize glucose differently at rest, an LBM-corrected SUV was used for BAT quantification.

SUV Threshold Correction to LBM Impacts Observed BAT Values. Adipose tissue is identified anatomically by its density in CT images [−300 to −10 Hounsfield units (HU)], but this criterion cannot distinguish BAT from WAT. Therefore, BAT is defined as having a metabolic activity above a fixed, investigator-defined PET SUV threshold that ranges from 1.0 to 2.0 g/mL (9, 19). Inconsistency with the typical SUV (based on body weight) for other metabolically active tissues (Fig. 1) prompted a study of the impact of an SUV threshold calculated based on LBM. The LBM-corrected SUV threshold [$SUV_{LBM} \geq (1.2\ g/mL)/(LBM\%)$] (11, 12) resulted in measured activated BAT volumes that were 3.7 ± 7.5% lower in lean subjects and 41.4 ± 21% lower in obese subjects (Fig. 1*C* and Fig. S1) compared with the fixed LBM-corrected SUV threshold (SUV_{TBM}) of ≥1.5 (20). BAT volume and activity differences between lean and obese subjects were statistically significant when the individual SUV_{LBM} thresholds were used, but not when the SUV_{TBM} threshold was used.

Table 1. Subject characteristics

Characteristic	Lean (n = 12)	Obese (n = 8)	P value*
Age, y	22.5 ± 4.9	28.8 ± 4.7	0.015
Height, cm	183.0 ± 7.0	183.1 ± 7.2	0.939
Weight, kg	77.8 ± 8.8	117.1 ± 12.0	<0.001
Fat mass, kg	16.2 ± 5.5	45.6 ± 9.5	<0.001
BMI, kg/m^2	23.2 ± 1.9	34.8 ± 3.3	<0.001
Lean to total mass ratio	0.75 ± 0.05	0.58 ± 0.05	<0.001
Lowest tolerable temperature, °C†	21.2 ± 1.6	20.2 ± 1.7	0.238
Mean skin temperature, °C†	29.9 ± 0.8	29.3 ± 0.9	0.270
Fasting plasma glucose, mg/dL†	92.4 ± 5.2	99.0 ± 11.1	0.231

Data are presented as mean ± SD.
*Using the Mann–Whitney U test.
†Before PET/CT imaging.

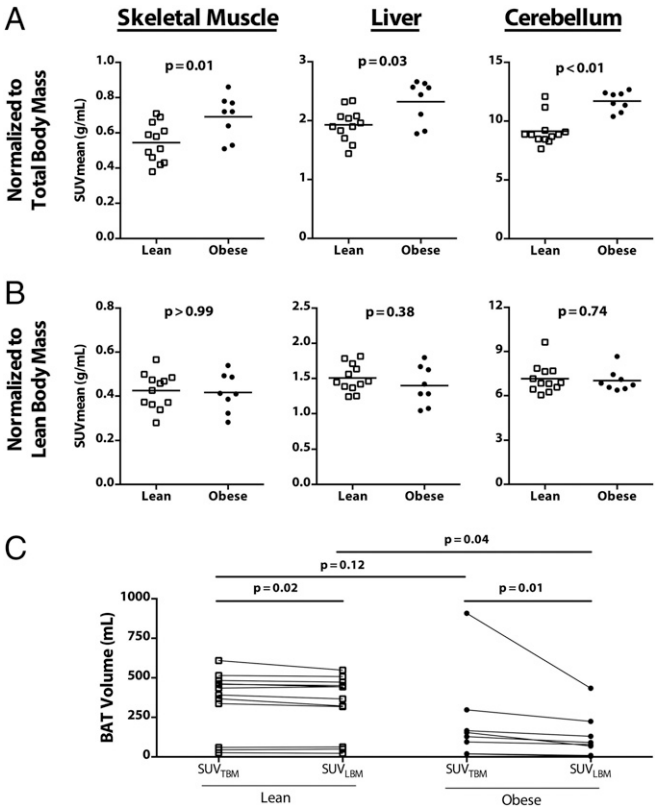

Fig. 1. (*A* and *B*) Comparison of SUV values of metabolically active tissues normalized to TBM (*A*) vs. LBM (*B*) as measured by DXA. ROIs were drawn on the right pectoralis major, segment VII of the right lobe of the liver, and the right cerebellum (tissue ROI locations in Fig. S3). (*C*) BAT volumes using SUV normalized to TBM vs. to LBM. SUV_{TBM} lower threshold, ≥1.5 g/mL for all subjects; SUV_{LBM} lower threshold, ≥1.2/ LBM% g/mL. #*P* values calculated by the Mann–Whitney U test. **P* values calculated using the paired t test.

Coronal ROI Selections Likely Overestimate BAT Volume Compared with Axial ROIs. We applied ROIs to quantify BAT using two different methods. A simple and commonly used method (8, 15, 21) is a 2D ROI defined in the coronal plane (2D-coronal), applied through the entire image volume. Alternatively, drawing individual ROI drawn on each axial PET slice allows for better selectivity, providing 3D insight (3D-axial). When two independent observers applied the 2D-coronal method, there was a strong interobserver correlation in the detected BAT volume (Fig. S2). When the same two observers used the 3D-axial selection criteria to 231 slices from a PET/CT image of a subject with highly visible ^{18}F-FDG uptake, the detected BAT

volume was also strongly correlated and differed by only 3.0%. Similar results were seen for interobserver differences in measured BAT activity (Fig. S2).

Using the slice-by-slice axial ROI selection method for BAT identification, we observed a 63 ± 16% reduction in measured whole-body BAT volume compared with the coronal ROI selection method in similar body compartments (Fig. 2*C*). Nevertheless, the two measures were highly correlated (Fig. 2*D*).

PET Image Resolution Impacts Observed Maximal Glucose Uptake in BAT. To examine the effect of PET image resolution on observed SUVs, we measured metabolic activity within seven tissue sites (Fig. S3) of subjects (n = 8) with detectable BAT metabolic activity in both supraclavicular and axillary regions. The SUVmax of BAT was considerably higher than that of five other tissues—subcutaneous white adipose tissue (scWAT), deltoid muscle, liver, myocardium, and cerebellum—independent of the image resolution (Fig. 3*A*). However, only the SUVmax of the supraclavicular and axillary BAT was higher when the 3.5-mm resolution images were smoothed to a resolution of 7.0 mm (1.95- and 2.26-fold, respectively) (Fig. 3*B*). These findings demonstrate the high metabolic capacity of BAT SUVmax: 62.1 ± 19.8 g/mL (10- to 50-fold more glucose uptake than scWAT (1.9 ± 0.9 g/mL) and greater than brain (15.3 ± 2.8 g/mL), heart (17.0 ± 6.9 g/mL), liver (3.9 ± 1.2 g/mL), and resting skeletal muscle (1.2 ± 0.5 g/mL)); however, they also show that it is inaccurate to directly compare BAT SUVmax values across images with differing PET resolutions. In contrast, the SUVmean of BAT values were similar in the 3.5-mm and 7.0-mm images (11.2 ± 1.2 vs. 12.3 ± 1.7 g/mL; P = 0.628). The differences in SUVmean values of other tissues ranged from −6.7% to 2.5%, and all were nonsignificant.

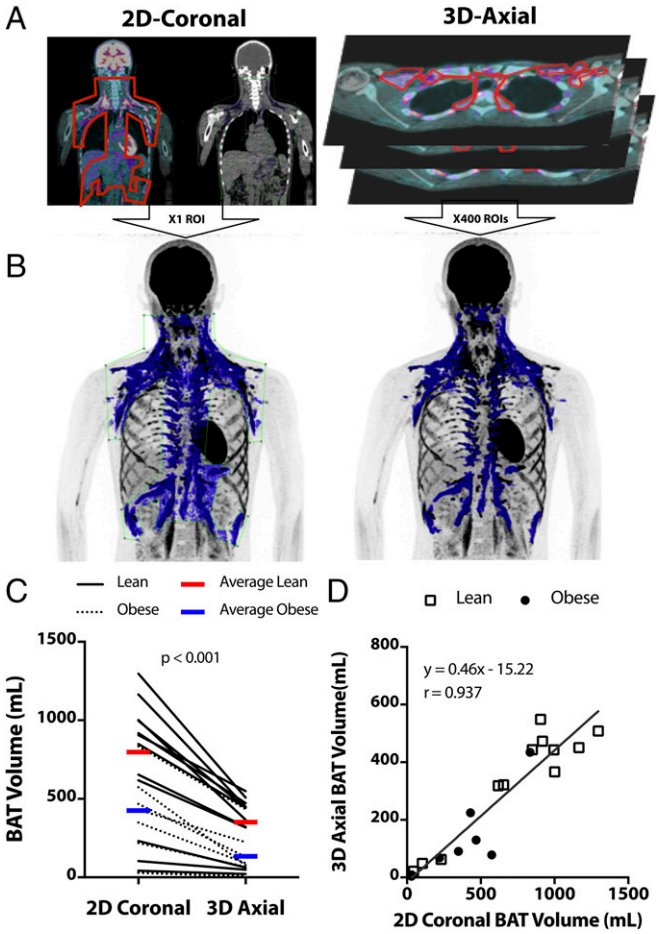

Fig. 2. Detected BAT volume quantified by axial and coronal ROI methods. (*A*) ROI selections for coronal and axial views (red lines). (*B*) Detected BAT shown in blue pixels. (*C*) Detected BAT volume for all subjects comparing coronal vs. axial methods. *P* value calculated by the Mann–Whitney *U* test. (*D*) Correlation between axial and coronal BAT volume quantifications.

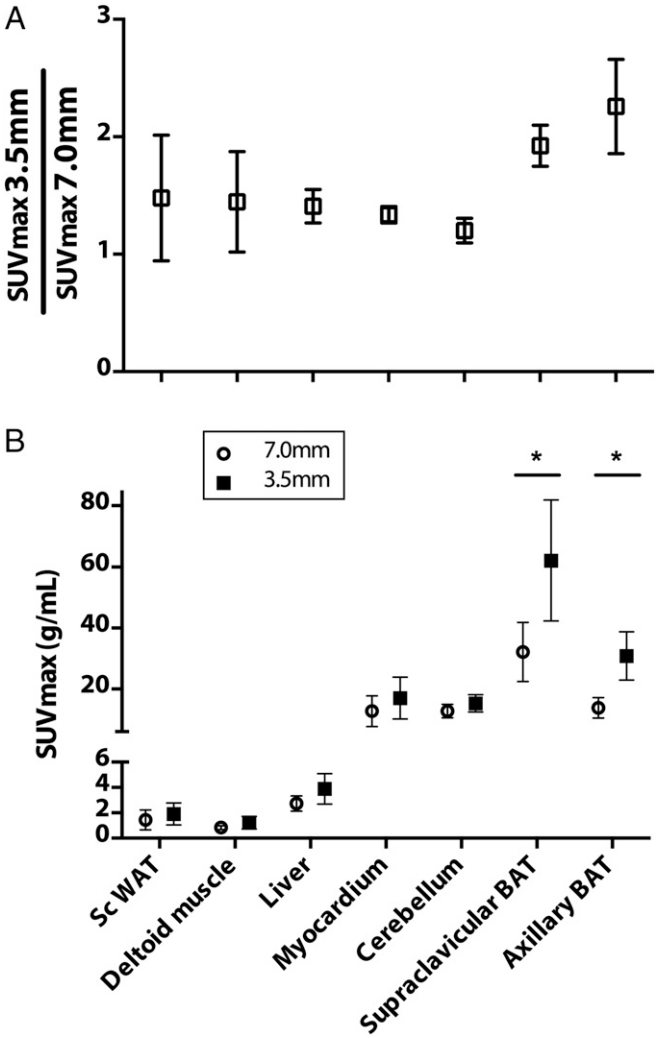

Fig. 3. Observed tissue SUVmax values of varying metabolic activity with PET resolutions of 7.0 and 3.5 mm (n = 8). Tissue ROI locations in Fig. S3. (*A*) Mean values with SD. *P < 0.05, two-way ANOVA. (*B*) Ratio of SUVmax obtained from 3.5 to 7.0 mm.

BAT Distribution. The distribution of BAT varied widely (Fig. 4 and Fig. S4) and was categorized by six anatomically distinct depots: cervical, supraclavicular, axillary, paraspinal, mediastinal, and abdominal. Of note, no activated BAT was seen in the large and typically white adipocyte-containing omental, mesenteric, and subcutaneous depots. The supraclavicular region contained the highest proportion of total body BAT volume. When combined with its contiguous fascial layers in the cervical and axillary regions, they collectively amounted to 66.6 ± 20% of the total BAT volume and 69.8 ± 19% of the total BAT activity. In addition, in subjects with the least amount of activated BAT, this single region contained nearly all the body's BAT (Fig. S4*A*).

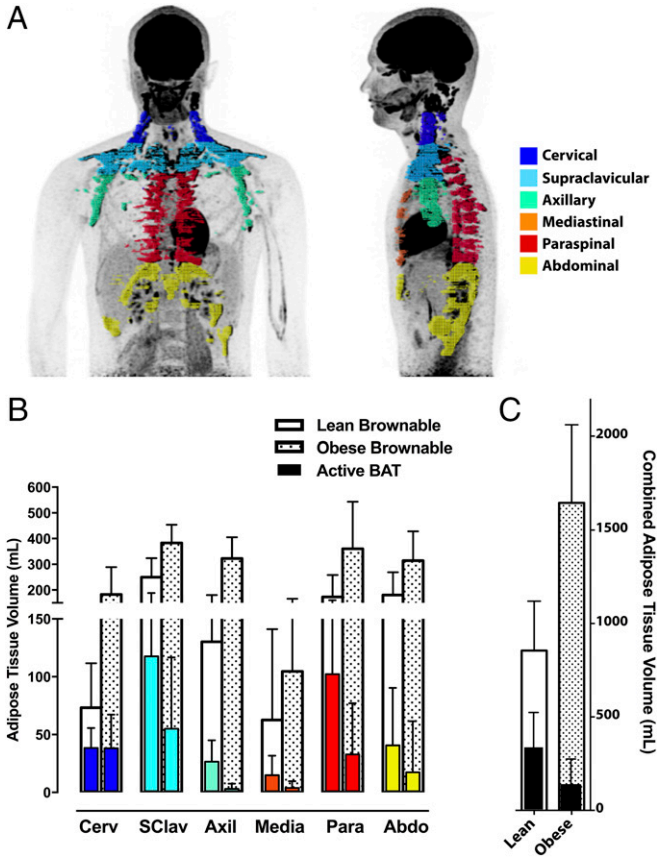

Fig. 4. Distribution and capacity of human BAT. (*A*) Regional distribution of BAT in six anatomic depots. (*B*) Average (SD) amount of activated and brownable inactive fat in the defined depots. (*C*) Summed active and brownable tissue in 12 lean subjects and 8 obese subjects. Empty and dotted bars in *B* and *C* represent volumes of the entire adipose tissue depots in which active BAT was found. The solid colored bars in *B* represent the volume of activated BAT within each adipose tissue depot, and the solid black bars in *C* represent the total activated BAT found in the body.

Calculation of Total Adipose Tissue in BAT Depots. We quantified the total amount of adipose tissue in each of the previously described BAT depots by applying the CT density thresholds without a PET SUV threshold (e.g., Fig. S5). The combined volume of the six depots ranged from 510 to 2,358 mL, including 26.1% ± 23.0% as activated BAT (Fig. 4 *B* and *C*). These depots of nonsubcutaneous adipose tissue amounted to 1.5% of the total body mass (4.3% of total fat mass). The supraclavicular regions had the highest ratio of activated BAT to total adipose tissue. Lean men had more BAT (Fig. 4*C*) and a higher proportion of adipose depot as activated BAT in all six depots (Fig. S4*B*).

BAT Quantification in a Case of Paraganglioma. To gain insight into the capacity for developing thermogenic adipocytes under chronic adrenergic stimulation, we quantified the regional total and brown fat volumes and the BAT activity in a patient with exceptionally high norepinephrine levels from a norepinephrine-secreting paraganglioma of the bladder (Fig. 5). PET/CT images were obtained in the absence of preceding cold exposure. scWAT and omental fat had lower metabolic activity (0.7 g/mL and 1.78 g/mL, respectively) and lower tissue density (−103 and −41 HU, respectively) than active BAT (11.03 g/mL and −24 HU) (Fig. 5). Total adipose tissue in all examined depots was 486 mL, of which 300 mL (62%) was active BAT (Table S1). The SUVmean of all BAT was 4.57 g/mL, SUVmax was 19.13, and BAT activity was 1,369 mL*SUVmean*(g/mL). Of note, 87% of the abdominal region was brown (161 mL of 185 mL) and contained more than one-half of the patient's BAT. In contrast, in the healthy lean subjects, BAT was most abundant in the supraclavicular depot (117.5 ± 72.1 mL, or 33.4 ± 9.9% of total detected BAT), and only 46 ± 28% of that region's adipose tissue was metabolically active.

Discussion

Human BAT is integrated among white adipocytes and often resides in narrow fascial layers adjacent to bone, skeletal muscle, and other organs, which hinders quantification of its volume and metabolic activity. There is no standard way to quantify BAT, making findings difficult to compare (16). BAT volumes have been reported to range from 14 mL to 665 mL (16), and thus BAT's functional relevance cannot be easily determined. Many of the previous studies quantifying BAT were retrospective and did not observe BAT under controlled, intentional stimulation (22, 23). In addition to the methodological variability, several physiological factors impact BAT image acquisition and measurement. Because ^{18}F-FDG enters metabolically active tissues disproportionately to WAT (24), the SUV threshold should be calculated based on body composition rather than based on body mass. When quantifying BAT in different regions, the 3D-axial ROI approach enables exclusion of apparent false-positives (due to ^{18}F-FDG uptake in nearby muscles and organs and/or artifacts inherent in image acquisition and processing) that a single ROI applied through the entire coronal plane cannot avoid. Finally, we show that PET image resolution has a substantial influence on observed BAT SUVmax. This suggests that SUVmax should not be the sole parameter for quantifying BAT activity. Although many factors influence the comparability of recent human data, our current findings combined with prior studies indicate that

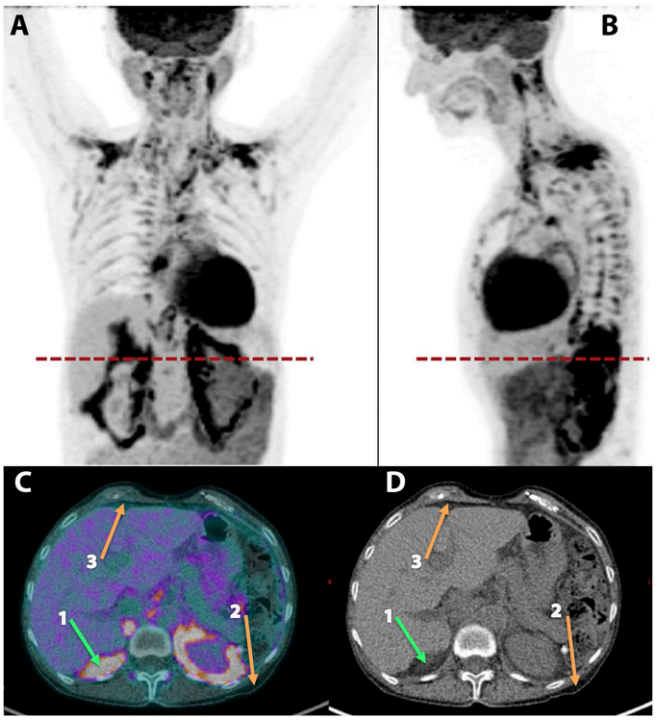

Fig. 5. scWAT and BAT in a patient with confirmed paraganglioma. (*A*) Frontal and (*B*) sagittal views of PET maximum intensity projection, with red lines indicating the axial slices shown in *C* and *D*. (*C*) Fused PET/CT image and (*D*) CT image alone showing 1, active BAT; 2, subcutaneous WAT; 3, inactive omental fat.

humans could have substantially more metabolically active BAT than is currently recognized.

In vitro and rodent studies have demonstrated that "browning," or increasing the content of thermogenic adipocytes of either brown or beige/brite lineage of WAT, is possible through either cold stimulation (25) or administration of an adrenergic stimulant (26). Chronic cold conditioning of human subjects also has been shown to increase BAT activity in several recent studies (27, 28). These lines of evidence have led some to postulate the energetic consequences of browning the entire WAT depot, including both visceral and subcutaneous fat (29). Our BATlas indicates that such an approach likely would be unsuccessful, because only certain adipose tissue depots seem capable of browning. Following whole-body adipose tissue inspection, only six specific anatomic regions that were previously been described as having BAT via imaging, biopsy, or dissection (30–32) were shown to have active BAT volume and metabolic activity in both the healthy cohort and the patient with paraganglioma. Therefore, we believe that the total fat in these depots (~1,100 mL) may represent a more reasonable estimate of the maximum achievable volume of BAT in adult subjects. In our non–cold-acclimated group of healthy subjects, only 50% of this maximum estimated volume was activated BAT in the individual with the highest percentage. However, in five of six brownable depots, one or more subjects had >80% as activated BAT. In addition, although on average lean men had higher BAT volumes, several obese men were found to have substantial quantities of BAT. Inferior regions, such as the abdominal and paraspinal regions, had lower proportions of cold-activated BAT, which appeared to be "recruited" only in subjects with >100 mL of BAT. This demonstrates the potential for more BAT to develop within these anatomically inferior and posterior depots when greater BAT volumes are achieved. Taken together, these observations suggest that most individuals do not achieve their maximal BAT content, and that obese men in particular may have a greater potential for expansion.

Pharmacologic activation of BAT via catecholamines also may be possible, given that patients with elevated plasma norepinephrine in the setting of pheochromocytoma/ paraganglioma experience browning of the entire retroperitoneal abdominal adipose tissue depot (33, 34). The patient with a paraganglioma in the present study examined with chronic norepinephrine stimulation was found to have 62% of his brownable depots as activated BAT. Of note, this distribution of BAT is opposite that seen in typical healthy adults, in whom most of the total BAT resides in the inferior depots. This pattern may reflect differences in source of the BAT-stimulating norepinephrine between these two classes of patients; neurosympathetic stimulation preferentially activates superior depots, whereas pelvic-based tumors release norepinephrine in to the plasma in proximity to the inferior abdominal depots.

Along with volume, the maximum activity of BAT is important for determining its capacity to contribute to metabolism. Because BAT uses fatty acids and glucose as fuel and measuring maximal activity levels in vivo is difficult, we made an estimate using rodent data. In rodent studies, BAT can have an enormous impact on energy expenditure (35) and fuel substrate consumption (36). Studies suggest that BAT may be responsible for up to one-third, or even more (37), of overall metabolic rate in some cold-acclimated species (38) while accounting for <2% of total body mass (33). In addition, rodent brown adipocytes appear to have similar cellular physiology and thermogenic capacity as human brown adipocytes (3, 39). In warm-acclimated rats, BAT can generate 112 cal/g*d (40). Analogously, a healthy young man described here with 250 mL of BAT can generate 25.5 kcal/d from activated BAT alone (38). If chronic stimulation by cold (25) or pharmacologic agents (41) increased BAT's thermogenic potential to that of a cold-acclimated rat, the same amount of BAT could generate 115.5 kcal/d. Finally, if our subjects were to activate their WAT in the brownable depots to its capacity volumetrically and metabolically, it could increase energy expenditure by >520 kcal/d. Although we have made several assumptions in this speculative analysis, this estimation further demonstrates the theoretical contribution of BAT to human energy balance.

This study has several limitations to. First, there is no gold standard for directly measuring the volume of total-body human BAT by anatomic methods, because of the heterogeneous mixing of brown adipocytes with white adipocytes in multiple, widely distributed fat depots. Therefore, we cannot verify the accuracy of our measurements. Our study would have greater impact if accompanied by site-specific biopsy specimens from the different adipose tissue depots, to assess, for example, the relative importance of brown and beige/brite adipocytes for expansion and activation and the potential for remodeling of the different cell types during chronic activation. In addition, it is not possible to distinguish between the number of brown adipocytes in a given unit of image volume vs. the other cell types that are not as thermogenic. However, it may be posited that the SUV is sufficient to indicate metabolic activity independent of the exact composition of a given volume, assuming proper image coregistration. This is due in part to the limitations of PET resolution. Although we report values to the nearest 1 mL, this is below the spatial resolution of the PET images. A more fundamental limitation is that this study relies on ^{18}F-FDG uptake as a biomarker for BAT thermogenesis, but the precise correlation between the two is not known. Finally, this study included only lean and obese young men. Nevertheless, the advances in image analysis presented here should be particularly applicable when moving toward measuring BAT volume and metabolic activity in other populations, such as women and men of different ages and fat distributions.

In summary, lean and obese young men have more cold-activated BAT than previously estimated. The distinct localization of BAT to the posterior regions of the neck, thorax, and abdomen may have physiological implications regarding the role and growth pattern of BAT in adult humans. Our three adjustments to PET/CT analysis—SUV correction for lean body mass, avoidance of false-positive determinations with careful axial ROI selection, and use of finer PET resolution—allowed for more detailed and reliable assessments of BAT volume and activity, particularly in subjects with wide ranges of body composition. Our findings raise the possibility that if BAT could be maximized to its volumetric and metabolic capacity, it would substantially affect energy metabolism in adult humans.

Materials and Methods

Study Protocol. Subjects (n = 12 lean, 8 obese) were recruited through ClinicalTrials.gov (National Institutes of Health protocol no. 12-DK-0097; ClinicalTrials.gov identifier NCT01568671) and underwent screening to determine eligibility. All subjects were age 18–35 y, were nonsmokers, had no metabolic or psychological conditions, and did not take any medications. Subjects provided written informed consent, and all experiments were approved by the Institutional Review Board of the National Institute of Diabetes and Digestive and Kidney Diseases. PET/CT images were obtained after 5 h of cold exposure at each subject's individualized lowest tolerable temperature on a day following an overnight fast. Subjects were dosed with 10 mCi of ^{18}F-FDG by i.v. injection 60–90 min before scan acquisition using a Siemens Biograph mCT (Siemens Healthcare).

PET/CT Image Analyses. PET/CT images were reconstructed into image voxels of 1.45 × 1.45 × 1.5 mm for PET and of 0.98 × 0.98 × 1.5 mm for CT. The PET images, with a spatial resolution of 3.5-mm full-width at half maximum (FHWM), were uploaded into ImageJ (42) for image processing, along with a lower-resolution version of each generated by smoothing with a 3D Gaussian kernel to obtain a FWHM of 7.0 mm. The PET/CT Viewer plug-in with features customized for BAT quantification was used in each of the subsequent analyses, Specific CT density ranges were used to identify fat (−300 to −10 HU) from air and other tissues (12). ^{18}F-FDG uptake (g/mL) in

each PET image voxel was quantified as an SUV initially normalized to the individual's total body mass. Both PET SUV and CT HU criteria were met to identify metabolically active adipose tissue.

For SUV normalized to LBM, we obtained the PET SUVmean for spherical ROIs for three reference tissues (deltoid, cerebellum, and segment VII of the liver) that were identified based on the anatomic location and specified tissue density. To validate the effect of LBM on SUV in non-BAT tissues, we applied the following correction to each of the SUVmeans: SUV*(LBM%). We chose these tissues because we expected no metabolic differences between lean and obese men.

For the BAT SUV lower threshold, whole-body BAT volume and activity were detected using a fixed threshold, $SUV_{TBM} = 1.5$ g/mL, and a threshold corrected for individually DXA-measured LBM, $SUV_{LBM} = (1.2 \text{ g/mL})/(\text{LBM\%})$ (11).

We applied ROIs to quantify whole-body BAT using two different methods. In the 2D-coronal method, similar to previously applied methods (15, 34), we identified significant ^{18}F-FDG tracer uptake using the coronal PET maximum intensity projection and the corresponding CT image for anatomic guidance. A single ROI was drawn in the coronal plane around prominent and distinguishable metabolically active fat, with an attempt to avoid nonfat areas of glucose uptake. This single ROI was applied to every coronal PET/CT slice in the anterior-posterior plane.

In the 3D-axial method, one ROI was created on each axial slice, carefully avoiding regions that were not metabolically active fat, to minimize false-positive detection. ROI selection began at the slice corresponding to vertebra C3, and continued inferiorly until the umbilicus (between vertebrae L3 and L4) was reached. All axial ROIs were summed to calculate total body BAT volume and activity, and SUVs were averaged to determine the SUVmean.

Brown Adipose Tissue Distribution. Using the axial ROI selection method and PET SUV_{LBM} threshold from the 3.5-mm slice images, we analyzed the distribution of BAT throughout the body. For the regional analyses, we segmented the detected BAT voxels in each subject into previously defined depots (15, 21) for which we defined anatomic landmarks: cervical (C3–C7), supraclavicular (C7–T3, anterior to the spine), axillary (an extension of the supraclavicular region; posterior to the mediastinum and anterior to the spine, T3–T8), mediastinal (most anterior BAT depot, T3–T12), paraspinal (T1–T12), and abdominal (T12–L4, including retroperitoneal). In the next analysis, total adipose tissue content was quantified by applying CT HU threshold of −300 to −10 in all ROIs found in each of the six BAT depots without an SUV threshold. Subcutaneous and mesenteric fat beyond each fascial layer were not included.

Statistical Analyses. Statistical tests were performed in GraphPad Prism 6 and R version 3.0.2. The nonparametric Mann– Whitney *U* test was used for comparisons between lean and obese subjects. Pearson correlation was used to identify relationships between ROI selection methods and coronal interobserver reproducibility. The χ^2 goodness-of-fit test was used to test interobserver reproducibility. MANOVA was performed to detect differences in regions of BAT between lean and obese. Two-way ANOVA detected within-subject differences in SUV. Statistical significance was determined by $P < 0.05$.

ACKNOWLEDGMENTS. We thank Marc Reitman for his contributions to the study design and manuscript preparation. We also thank the nursing staff and dieticians of the Clinical Metabolic Research Unit at the National Institutes of Health's Clinical Center in Bethesda, MD, for their interactions with and care for all research participants during their inpatient stays. This work was supported by Intramural Research Program of the National Institute of Diabetes and Digestive and Kidney Diseases Grants Z01 DK071014 (to K.Y.C.) and DK075116-02 (to A.M.C.).

1. Cannon B, Nedergaard J (2004) Brown adipose tissue: Function and physiological significance. *Physiol Rev* 84:277–359.
2. Wu J, et al. (2012) Beige adipocytes are a distinct type of thermogenic fat cell in mouse and human. *Cell* 150:366–376.
3. Porter C, et al. (2016) Human and mouse brown adipose tissue mitochondria have comparable UCP1 function. *Cell Metab* 24:246–255.
4. Cypess AM, et al. (2013) Anatomical localization, gene expression profiling and functional characterization of adult human neck brown fat. *Nat Med* 19:635–639.
5. Lidell ME, et al. (2013) Evidence for two types of brown adipose tissue in humans. *Nat Med* 19:631–634.
6. Waldén TB, Hansen IR, Timmons JA, Cannon B, Nedergaard J (2012) Recruited vs. nonrecruited molecular signatures of brown, "brite," and white adipose tissues. *Am J Physiol Endocrinol Metab* 302:E19–E31.
7. Orava J, et al. (2011) Different metabolic responses of human brown adipose tissue to activation by cold and insulin. *Cell Metab* 14:272–279.
8. Chen KY, et al. (2013) Brown fat activation mediates cold-induced thermogenesis in adult humans in response to a mild decrease in ambient temperature. *J Clin Endocrinol Metab* 98:E1218–E1223.
9. Ouellet V, et al. (2012) Brown adipose tissue oxidative metabolism contributes to energy expenditure during acute cold exposure in humans. *J Clin Invest* 122:545–552.
10. Poekes L, Lanthier N, Leclercq IA (2015) Brown adipose tissue: A potential target in the fight against obesity and the metabolic syndrome. *Clin Sci (Lond)* 129:933–949.
11. Cypess AM, Haft CR, Laughlin MR, Hu HH (2014) Brown fat in humans: Consensus points and experimental guidelines. *Cell Metab* 20:408–415.
12. Chen KY, et al. (2016) Brown Adipose Reporting Criteria in Imaging STudies (BARCIST 1.0): Recommendations for standardized FDG-PET/CT experiments in humans. *Cell Metab* 24:210–222.
13. Soret M, Bacharach SL, Buvat I (2007) Partial-volume effect in PET tumor imaging. *J Nucl Med* 48:932–945.
14. Adams MC, Turkington TG, Wilson JM, Wong TZ (2010) A systematic review of the factors affecting accuracy of SUV measurements. *AJR Am J Roentgenol* 195:310–320.
15. Cypess AM, et al. (2009) Identification and importance of brown adipose tissue in adult humans. *N Engl J Med* 360:1509–1517.
16. van der Lans AAJJ, et al. (2014) Cold-activated brown adipose tissue in human adults: Methodological issues. *Am J Physiol Regul Integr Comp Physiol* 307:R103–R113.
17. Yoneshiro T, et al. (2011) Brown adipose tissue, whole-body energy expenditure, and thermogenesis in healthy adult men. *Obesity (Silver Spring)* 19:13–16.
18. Wahl RL, Jacene H, Kasamon Y, Lodge MA (2009) From RECIST to PERCIST: Evolving considerations for PET response criteria in solid tumors. *J Nucl Med* 50:122S–150S.
19. Matsushita M, et al. (2014) Impact of brown adipose tissue on body fatness and glucose metabolism in healthy humans. *Int J Obes* 38:812–817.
20. Vosselman MJ, et al. (2013) Brown adipose tissue activity after a high-calorie meal in humans. *Am J Clin Nutr* 98:57–64.
21. Lee P, et al. (2014) Temperature-acclimated brown adipose tissue modulates insulin sensitivity in humans. *Diabetes* 63:3686–3698.
22. Ouellet V, et al. (2011) Outdoor temperature, age, sex, body mass index, and diabetic status determine the prevalence, mass, and glucose-uptake activity of 18F-FDG-detected BAT in humans. *J Clin Endocrinol Metab* 96:192–199.
23. Gerngroß C, Schretter J, Klingenspor M, Schwaiger M, Fromme T (2017) Active brown fat during 18FDG-PET/CT imaging defines a patient group with characteristic traits and an increased probability of brown fat redetection. *J Nucl Med*, 10.2967/jnumed.116.183988.
24. Zasadny KR, Wahl RL (1993) Standardized uptake values of normal tissues at PET with 2-[fluorine-18]-fluoro-2-deoxy-D-glucose: Variations with body weight and a method for correction. *Radiology* 189:847–850.
25. Frontini A, Cinti S (2010) Distribution and development of brown adipocytes in the murine and human adipose organ. *Cell Metab* 11:253–256.
26. Bartelt A, Heeren J (2014) Adipose tissue browning and metabolic health. *Nat Rev Endocrinol* 10:24–36.
27. Hanssen MJW, et al. (2016) Short-term cold acclimation recruits brown adipose tissue in obese humans. *Diabetes* 65:1179–1189.
28. Blondin DP, et al. (2014) Increased brown adipose tissue oxidative capacity in cold-acclimated humans. *J Clin Endocrinol Metab* 99:E438–E446.
29. Kern PA, et al. (2014) The effects of temperature and seasons on subcutaneous white adipose tissue in humans: Evidence for thermogenic gene induction. *J Clin Endocrinol Metab* 99:E2772–E2779.
30. Heaton JM (1972) The distribution of brown adipose tissue in the human. *J Anat* 112:35–39.
31. Zingaretti MC, et al. (2009) The presence of UCP1 demonstrates that metabolically active adipose tissue in the neck of adult humans truly represents brown adipose tissue. *FASEB J* 23:3113–3120.
32. Virtanen KA, et al. (2009) Functional brown adipose tissue in healthy adults. *N Engl J Med* 360:1518–1525.
33. Sondergaard E, et al. (2013) Case report: Chronic adrenergic stimulation induces brown adipose tissue differentiation in visceral adipose tissue. *Endocr Abstracts* 32:P213.
34. Iyer RB, Guo CC, Perrier N (2009) Adrenal pheochromocytoma with surrounding brown fat stimulation. *AJR Am J Roentgenol* 192:300–301.
35. Foster DO, Frydman ML (1978) Brown adipose tissue: The dominant site of nonshivering thermogenesis in the rat. *Experientia Suppl* 32:147–151.
36. Bartelt A, et al. (2011) Brown adipose tissue activity controls triglyceride clearance. *Nat Med* 17:200–205.
37. Abreu-Vieira G, Xiao C, Gavrilova O, Reitman ML (2015) Integration of body temperature into the analysis of energy expenditure in the mouse. *Mol Metab* 4:461–470.
38. Foster DO (1984) Quantitative contribution of brown adipose tissue thermogenesis to overall metabolism. *Can J Biochem Cell Biol* 62:618–622.
39. Chakrabarty K, Chaudhuri B, Jeffay H (1983) Glycerokinase activity in human brown adipose tissue. *J Lipid Res* 24:381–390.
40. Smith RE, Roberts JC (1964) Thermogenesis of brown adipose tissue in cold-acclimated rats. *Am J Physiol* 206:143–148.
41. Cypess AM, et al. (2015) Activation of human brown adipose tissue by a β3-adrenergic receptor agonist. *Cell Metab* 21:33–38.
42. Barbaras L, Tal I, Palmer MR, Parker JA, Kolodny GM (2007) Shareware program for nuclear medicine and PET/CT PACS display and processing. *AJR Am J Roentgenol* 188:W565–8.